Indian Journal of Engineering & Materials Sciences
Vol. 27, April 2020, pp. 288-299

Anchoring the CFRP strengthening of concrete bridge decks: A comparison of methods

Tian Shuai[a*], Miao Zhenkun[b] & Sun Bo[c]

School of Civil Engineering, Liaoning University of Science and Technology, Anshan 114051, China.

Received: 26 March 2019 ; Accepted:11 March 2020

Debonding failures are a common problem in concrete bridge decks strengthened with adhesively attached carbon-fibre reinforced polymer (CFRP) strips. Accordingly, in this study, rectangular concrete slabs strengthened with CFRP have been experimentally evaluated to simulate the strengthening of T-beam and box girder slabs. The resulting static load data have been used to compare the effects of four different anchoring methods in terms of crack distribution, deflection, reinforcing steel strain curve, and CFRP strain distribution. The most suitable bridge deck strengthening anchoring method has been then identified and analysed using extant strengthening design methods. The results show that the most practical anchoring method is the use of open CFRP strips attached with concentrated adhesive. The findings of this study indicate that when strengthening T-girder bridges, more than two CFRP anchorage strips should be evenly spaced within the extension of the anchorage length, while for box girder bridges, even more evenly spaced strips should be used. This research and its conclusions can be used as a reference for the improved design of bridge deck strengthening.

Keywords: Bridge engineering, CFRP strengthening, Bridge deck strengthening, Strengthening anchoring method

1 Introduction

In recent years, reports of longitudinal cracking in concrete highway bridge decks has increased, including typically serious damage on the Bangabandhu Bridge in Bangladesh and the Guanghua Bridge in Hubei, China. Additionally, New Zealand and Australia have reported typical longitudinal cracking of concrete bridge decks. Longitudinal cracking in concrete bridge decks is mostly caused by vehicle loads and temperature stress. If bridge deck longitudinal cracking is sufficiently serious and not addressed in a timely manner, the normal use and operation of the bridge with be detrimentally affected [1–3].

The use of carbon-fibre reinforced polymer (CFRP) in bridge deck strengthening is fairly new [4,5]. As a retrofitting material, transverse CFRP can be adhered to concrete bridge decks in the appropriate locations to constrain the development of longitudinal cracks. A waterproof layer is then placed atop the CFRP and asphalt pavement placed on the deck to provide improved reinforcement. In this way, the service life of a bridge deck can be prolonged.

However, as a new material being applied to bridge deck strengthening, CFRP still exhibits many potential problematic behaviours that need to be studied and resolved [6,7]. Currently, research on CFRP debonding failures and anchorage mechanisms is primarily focused on concrete beam strengthening[8-13]. The relevant standard for the CFRP strengthening of bridge decks is quite lacking, and research on the process of CFRP debonding failure and anchoring mechanisms remains insufficient [14–19]. As a result, the safety and reliability of bridge deck reinforcement using CFRP requires further investigation. Accordingly, the objective of this study is to evaluate the debonding failure of CFRP deck reinforcement according to anchoring method. The results of this study are of great significance for improving deck reinforcement design and application to engineering structures.

2 Strengthening Design

2.1 Bridge Deck Strengthening Design

At present, most bridge decks are multi-span continuous one-way slabs: the roof slabs of box girders utilise a "one-time-concreting" structure and the flange slabs of T-beams utilise a "cast-in-situ wet joint, double casting" structure. There are two methods of strengthening against longitudinal cracking in a multi-span continuous one-way slab: negative moment area strengthening and positive

*Corresponding author (E-mail: tian_shuai129@126.com)

moment area strengthening, shown in Figs. 1(a) and (b), respectively.

When strengthening bridge decks in a negative moment area, the CFRP should be attached to the top of the slab over a support and between two moment inflection points such that the cut-off point of the CFRP is located in a positive moment area; reliable anchoring measures should be taken within this extended length. When strengthening bridge decks in a positive moment area, the CFRP should be attached to the bottom of the deck between supports such that the cut-off point of the CFRP is located in a negative moment area, where again, reliable anchoring measures should be taken.

At present, the transverse deck span of typical T-beam bridge is about 1.8 to 2.5 m long with a thickness of more than 14 cm[20]; the transverse deck span of a typical box-beam bridge is about 3 to 6 m long with a thickness of 20 to 25 cm[20]. Based on these data, experimental specimens were constructed to a scale of 1:1.5 and 1:2.5 to represent T-beams and box-beams, respectively. When designing the strengthening of a statically indeterminate beam (or slab), the spans between each two inflection points are usually simplified into simply supported beams. By this principle, the test specimens were made to be simply supported slabs 1600 mm long, 400 mm wide, and 100 mm thick to simulate deck strengthening in the areas of negative and positive bending tension. The CFRP strips used were 1.4 mm thick, 100 mm wide, had a tensile strength greater than 2300 MPa, and an elastic modulus greater than 150 GPa. The CFRP adhesive used had a tensile strength greater than 25 MPa, an elastic modulus greater than 2500 MPa, a bending strength greater than 30 MPa, and a compressive strength greater than 70 MPa. The slab specimens were cast from C30 concrete with an equal reinforcement ratio of 0.98% constituted by 5-10 mm HRB335 screw-thread steel in the tension area. In the transverse direction, a total of 11 steel bars of the same diameter were distributed in the slabs. These specimens were used to simulate bridge deck strengthening according to the requirements of the strengthening design code for highway bridges (JTG/TJ22-2008) by fixing CFRP onto the desired face of the slab. The concrete slab strengthening design is shown in Fig. 2.

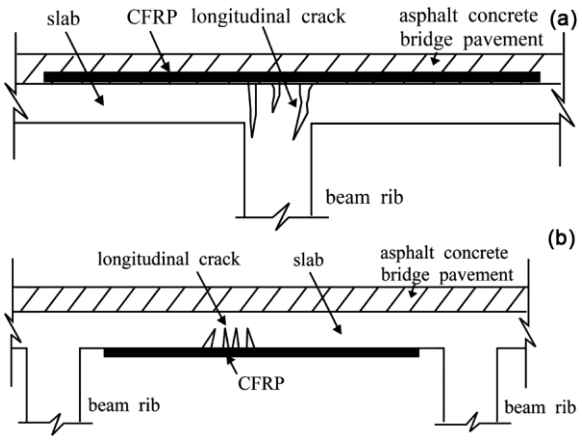

Fig. 1 — Types of bridge deck strengthening (a) Negative moment area strengthening and (b) Positive moment area strengthening.

2.2 Anchoring Method

Due to the predilection of CFRP materials to debond, a strengthened bridge deck behaves in an obviously brittle way. As the CFRP debonds, the utilization rate of the strengthening material falls too low to meet the strengthening demand, so it is particularly important to determine suitable methods for anchorage. It is important to note that the bending strengthening of a slab is different from that of a beam. Current research has demonstrated that a slab is more likely to exhibit debonding caused by central cracks, and that end-section debonding is a potential failure mode [15]. As a result, in bridge deck strengthening, CFRP strip anchorages must be used perpendicular to the direction of primary strengthening to effectively prevent debonding caused by central cracks. These CFRP strips should thus be connected at inflection points where one-way bending moment is present, and it should be ensured that the distance between sets of CFRP anchorage strips is not excessively large. Based on the above considerations,

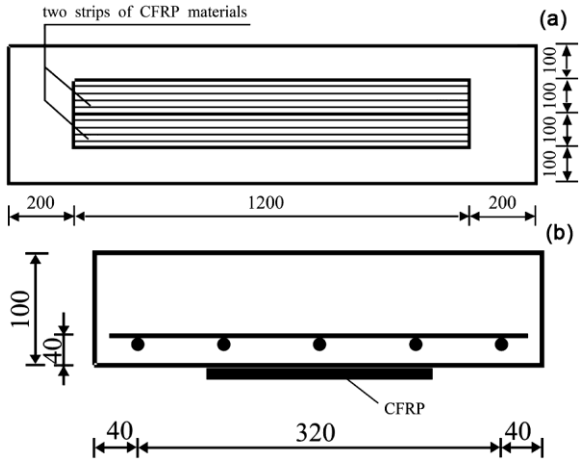

Fig. 2 — CFRP strengthening design (a) Plane view and (b) Section view (in mm).

in this study, the length along the primary CFRP strengthening between anchorage strips was set between 750 and 800 mm.

The slab specimens were divided into control and test specimens and statically loaded. The CFRP-strengthened specimens were designed using the four different anchoring methods described in the strengthening design code for highway bridges (JTG/TJ22-2008): open concentrated CFRP strips attached by adhesive, open CFRP strips attached in intervals by adhesive, closed-looped concentrated CFRP strips attached by adhesive, and steel strips attached by bolts, represented in this paper as M_1, M_2, M_3, and M_4, respectively. Methods M_1 and M_2 were tested together in Combination I, while methods M_3 and M_4 were tested together in Combination II, as shown in Fig. 3. A total of six rectangular reinforced concrete slab specimens were tested with the anchoring methods and main parameters shown Table 1.

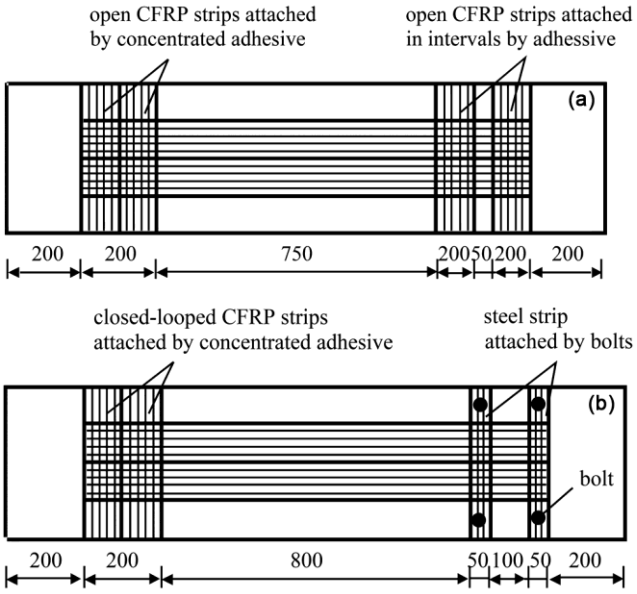

Fig. 3 — Anchoring methods (a) Combination I and (b) Combination II (in mm).

3 Experimental Methods and Procedures

3.1 Experimental Methods

This experiment compared the improvement in the bending capacity and behaviour of a rectangular reinforced concrete slab when strengthened along its span under single-point and third-point symmetric loadings using different anchoring methods. The loading apparatus used can be seen in Fig. 4. In the loading apparatus, the side of the slab with CFRP attached was placed facing downward between supports spaced at 1400 mm. Under midspan single-point loading, load was applied through a full slab-width 160-mm deep steel I-section and a 5 mm

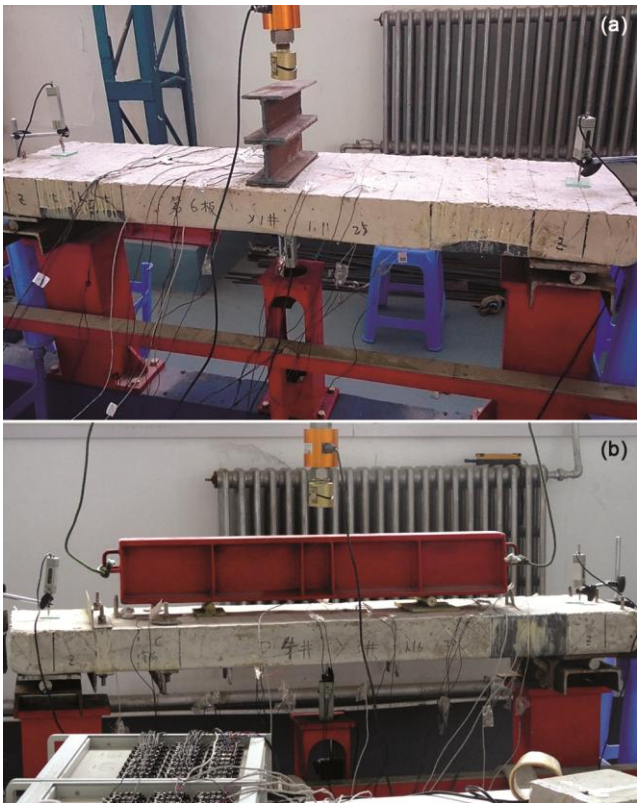

Fig. 4 — Slab specimen loading apparatus (a) Midspan single-point loading and (b) Third-point symmetric loading.

Table 1 — Main parameters of slab specimens.

Group	Slab name	Strengthening method	Anchoring method	Loading mode	Remarks
Control specimen	C_1 / C_2	None	None	Midspan single-point loading / Third-point loading	Not strengthened
Static specimen Group A	D_1 / D_2	Two CFRP strips attached lengthwise	Combination I / Combination II	Midspan single-point loading	Compares bending failure under different anchoring methods
Static specimen Group B	S_1 / S_2	Two CFRP strips attached lengthwise	Combination I / Combination II	Third-point loading	Compares bending shear failure under different anchoring methods

rubber pad. Under the symmetric third-point loading, load was applied through a steel distribution beam to rollers and plates located 600 mm apart. The distance from the load application point of the distribution beam to the slab support was 400 mm. To obtain data describing the concrete strain, CFRP strain, reinforcing steel strain, midspan deflection, and support settlement under load, the instruments used in the experiments included a dynamic and static strain measurement system, a tension/compression sensor, a displacement sensor, and a screw jack. When measuring strain, the effects of temperature were taken into account. Displacement sensors were installed at the midspan and end supports. The final midspan deflection reported for the experimental slabs has any support settlement deducted. A concrete strain gauge was pasted along the midspan of the slab side and a metal strain gauge was pasted on the main bearing steel bars. The metal strain gauge was placed before concrete pouring. A certain number of metal strain gauges were also arranged on the CFRP surface along the length of the experimental slabs at a distance of 200 mm.

3.2 Experimental Procedure

This experiment used a 300 kN hydraulic jack to apply the desired load. Prior to the experiment, a 5-kN pre-load was applied to the specimen to eliminate the space between the loading and support devices and the slab, the equipment was checked for effectiveness and sensitivity, and then the formal loading program was conducted. Under the formal loading program, the maximum load applied was determined by loading to slab failure, defined as the occurrence of steel yielding, concrete crushing, CFRP debonding, or hydraulic jack unloading after additional anchorage damage. The load was periodically stabilised to ensure that accurate data was obtained. The deflection of the section, strain in the tensile steel bars and CFRP, and compression in the concrete were recorded.

4 Results and Analysis

4.1 Crack Development

During the static loading process, a magnifying glass was used to determine the occurrence, development, and distribution of cracks in the slabs, and the observed crack maps are shown in Fig. 5. The numbers at the crack tips in Fig. 5 give the corresponding applied jack load in kN once the cracks had developed to their respective ends. Note that Fig. 5 is drawn to a horizontal to vertical scale of 1:2, and the grid drawn by the dashed lines forms 100 mm × 50 mm cells.

As shown in Fig. 5(a), under single-point loading, Slab C_1 developed a main bending crack, branch cracks at the tip of the main crack, and root cracks near the steel. The main bending crack appeared first, and the branch cracks at the tip of this main crack developed following a similar inclination angle. As can be seen in Fig. 5(d), under third-point symmetric loading, Slab C_2 exhibited a bending shear inclined crack in the bending shear zone, a main bending crack in the pure bending zone, branch cracks in the middle of the bending shear inclined crack, and root cracks near the steel. The bending shear inclined crack and the main bending crack developed at the same time, following an obvious trend. Under single-point loading, shown in Figs. 5(b) and 5(c), CFRP-strengthened slab Group A (D_1 and D_2) exhibited a main bending crack, branch cracks at the tip of the main crack, and root cracks near the steel and CFRP. There were more cracks for this group than for Slab C_1, and the branch cracks at the tip of the main crack were very obvious. Under third-point symmetric loading, slab Group B (S_1 and S_2) exhibited a bending shear inclined crack in the bending shear zone, a bending crack in the pure bending zone, branch cracks in the middle of the main crack, root cracks near the steel, and secondary cracks near the CFRP. There were more cracks for this group than for C_2, and it was obvious that the bending shear inclined crack was the main crack contributing to the slab specimen failure.

As can be seen in Fig. 5, the control specimen exhibited fewer cracks and the distance between cracks was larger than for the strengthened specimens. Comparing the distribution of cracks in the strengthened specimens under the different loading patterns, it was obvious that the bending cracks in the middle of the slabs caused the observed failures, and that cracks in the M_1 anchorage were smaller than those in the M_2 anchorage, indicating that the M_1 anchoring method was more effective. The cracks in the M_3 anchorage were smaller than those in the M_4 anchorage, indicating that the M_3 anchoring method was more effective. These conclusions can also be obtained from the load in the CFRP at debonding failure of the slab specimens. In general, the different anchoring methods can be arranged in order of decreasing effectiveness as $M_3 > M_1 > M_4 > M_2$.

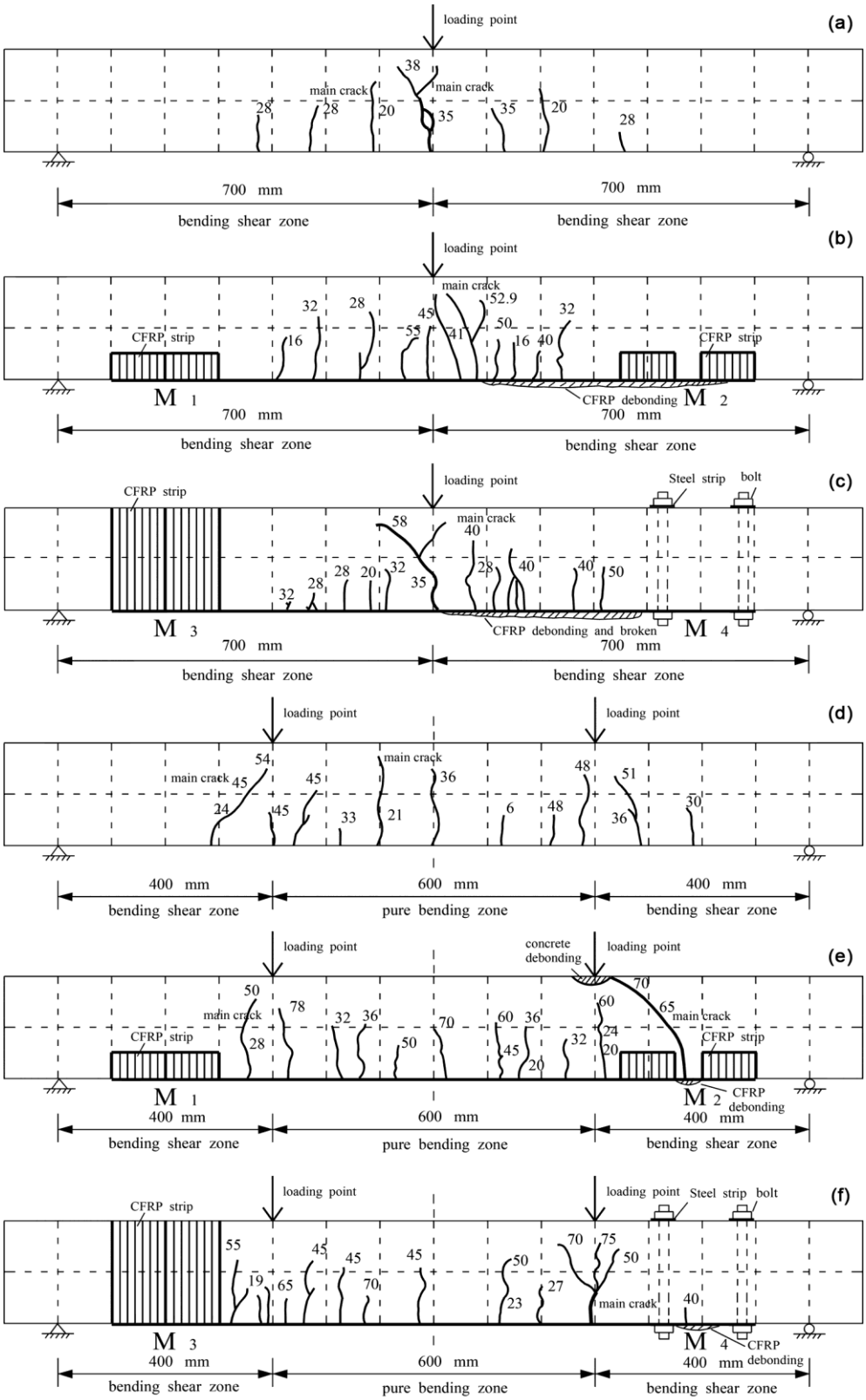

Fig. 5 — Crack distribution after damage in (a) Control Slab C_1 (single-point loading), (b) Strengthened Slab D_1 (single-point loading), (c) Strengthened Slab D_2 (single-point loading), (d) Control Slab C_2 (third-point loading), (e) Strengthened Slab S_1 (third-point loading) and (f) Strengthened Slab S_2 (third-point loading).

4.2 Analysis of Load–Deflection Curves at Midspan

As shown in the load–deflection curves of the slab specimens under single-point loading in Fig. 6(a), the cracking load of Slab C_1 was low and its rigidity was poor, while the cracking load of Group A was higher than that of control Slab C_1. After cracking, the tensile strength of CFRP postponed further shifting of the section neutral axis, and the specimen rigidity slowly decreased. In the late stage of loading, the anchoring methods of Slab D_2 were shown to be effective, as manifested in the small displacement and high rigidity of the slab specimen. Clearly, the anchoring methods evaluated in D_1 were not as effective as those in D_2.

As shown in the load–deflection curves of the slab specimens under third-point loading in Fig. 6(b), the cracking load of Slab C_2 was almost as the same as that of Group B. When the applied load was low, the slab specimens were in the elastic stage. Once the concrete in the Group B slabs stopped contributing to it, the tensile force was shared by the steel and CFRP. As the load increased, the CFRP gradually played an increasing role in constraining the cracking of the concrete, manifesting as an improvement in rigidity. In the late stage of loading, the anchoring methods of Slab S_1 were generally as effective as those of Slab S_2, as manifested in the small displacement and high rigidity of the slab specimen.

Overall, comparing the load–deflection curves under different loading schemes, M_3 and M_4 can be observed to be superior anchoring methods to M_1 and M_2.

4.3 Analysis of Reinforcing Steel Load–Strain Curves

As can be observed in the reinforcing steel load–strain curve for single-point loading shown in Fig. 7(a), the steel in the specimens of Group A and Slab C_1 all yielded. Under the same load, the steel strains in Slabs D_1 and D_2 were relatively small, indicating that the CFRP strengthening shared some of the force normally borne by the steel reinforcement. According to the curve trend, the anchoring methods applied in D_2 were more effective than those applied in D_1.

As can be observed in the reinforcing steel load–strain curve for third-point loading shown in Fig. 7(b), the reinforcing steel in C_2 yielded, while the

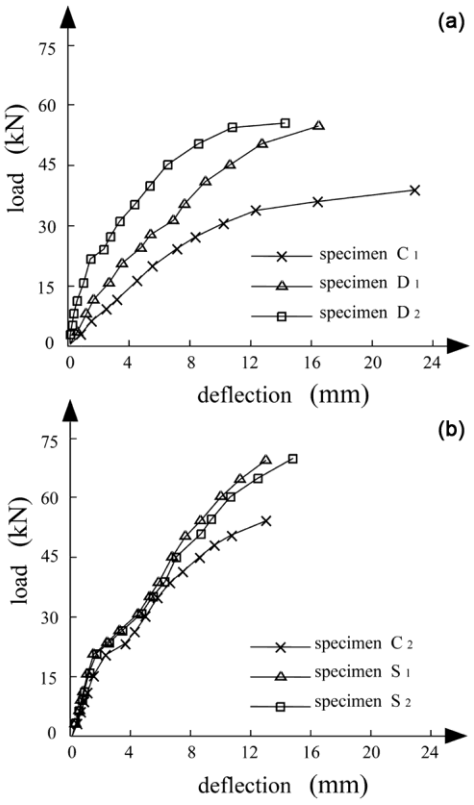

Fig. 6 — Load–deflection curves for (a) Single-point loading and (b) Third-point loading.

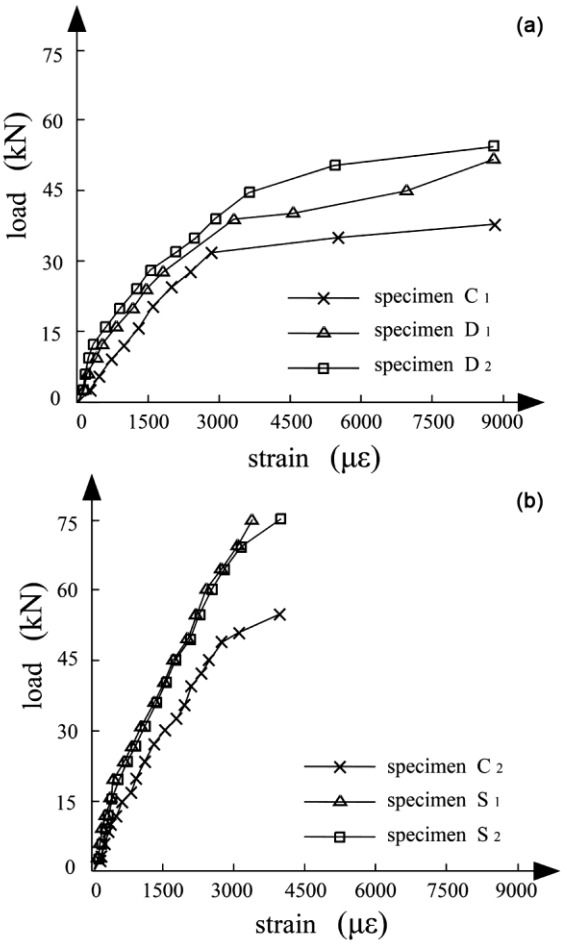

Fig. 7 — Reinforcing steel load–strain curves under (a) Single-point loading and (b) Third-point loading.

reinforcing steel in S_2 showed only subtle evidence of yielding. Under the same load, the steel strains in Slabs S_1 and S_2 were very close, and lower than in C_2. This again indicates that the CFRP strengthening shared some of the force normally borne by the steel reinforcement. According to the curve trend, the anchoring methods applied in S_1 were as good as those applied in S_2.

Overall, comparing the steel load–strain curves under different loading schemes, M_3 and M_4 are clearly more effective than M_1 and M_2.

4.4 Analysis of Strain Distribution in CFRP under Different Loads

The strain distribution curves of the CFRP in the strengthened slabs under single-point loading are shown in Figs. 8(a) and (b), and those under third-point loading are shown in Figs. 8(c) and (d). In general, the CFRP strengthening shared tensile force with the reinforcing steel very well.

When the load applied to Slab D_1 was 54.9 kN, the CFRP strain at midspan reached its peak of 10 000 με. The strain–displacement curve is steeper on the left side of the peak than on the right side, indicating that anchoring method M_1 more effectively limited CFRP debonding resulting from the development of a central bending crack than method M_2. When the load applied to Slab D_2 was 56.7 kN, the peak strain in the CFRP of 6300 με appeared to the right of midspan, while under an applied load of 45 kN, the CFRP strain at midspan was the largest instead. This change indicates that anchoring method M_3 more effectively limited CFRP debonding resulting from the development of a central bending crack than method M_4. Comparing the strain distribution in the CFRP of slabs D_1 and D_2 under their ultimate loads, it is obvious that CFRP strain everywhere in Slab D_1 was higher than in Slab D_2. Additionally, the strain distribution in Slab D_1 was steeper than in Slab D_2. Therefore, the different anchoring methods can be listed in order of decreasing effectiveness as $M_3 > M_4 > M_1 > M_2$.

When the load applied to Slab S_1 reached 69.9 kN, the strain distribution in the CFRP in the pure bending zone was an approximately horizontal line, indicating that the CFRP in S_1 shared the tension force with the reinforcing steel quite well. Under the M_2 anchoring method, the CFRP strain in the bending shear zone between the two CFRP anchorage strips was still very high. In this anchorage interval, the development of an inclined central bending shear crack caused CFRP debonding, which could extend beyond the CFRP anchorage strips and cause the strengthening to fail.

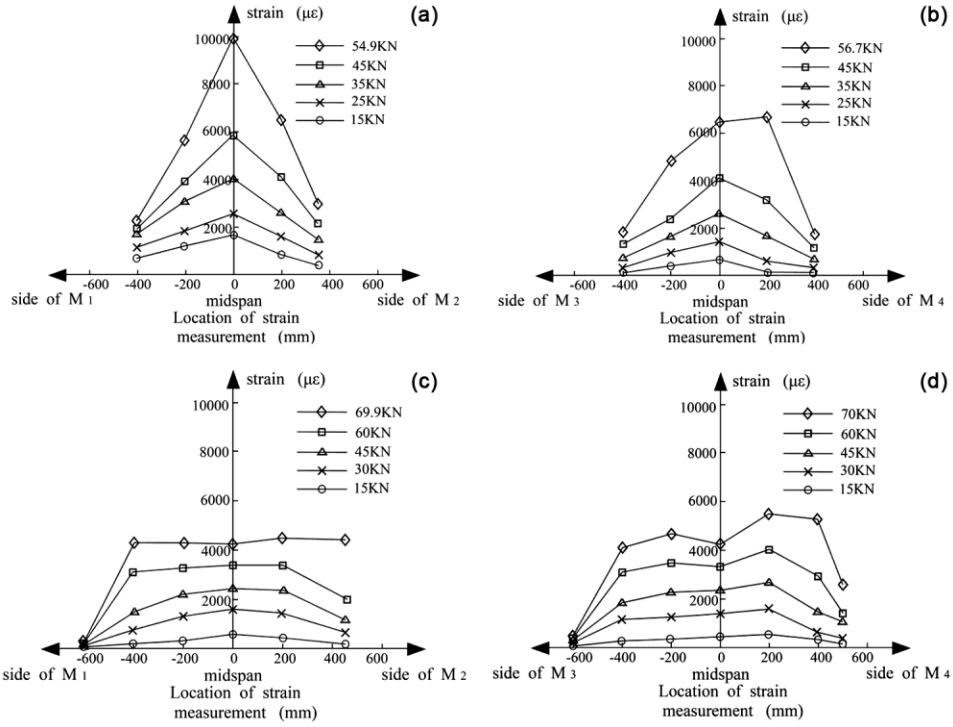

Fig. 8 — Strain distribution in CFRP under different loads for (a) Strengthened Slab D_1, (b) Strengthened Slab D_2, (c) Strengthened Slab S_1 and (d) Strengthened Slab S_2.

This indicates that the effect of anchoring method M_1 was better than that of M_2. When the load applied to Slab S_2 reached 70 kN, the strain distribution in the CFRP increased suddenly on the right side of the pure bending zone. This indicates that an inclined central bending shear crack caused the CFRP to debond and could extend beyond the steel strip anchorage. Clearly, the anchorage effect of the steel strips in inhibiting CFRP debonding was not ideal, and thus the effect of M_3 was better than that of M_4. Comparing the strain distribution in the CFRP strips of slabs S_1 and S_2 under every applied load, it is obvious that influence of anchoring methods M_1 and M_2 on the distribution of CFRP strain is quite similar, and that the anchoring effect of methods M_1 and M_3 is better than that of methods M_2 and M_4.

4.5 Effect of Anchoring Methods on specimen Debonding Failures

Different anchoring methods have different influences on the occurrence and nature of CFRP debonding failure. Among the four evaluated anchoring methods, the behaviour of the steel strips in M_4 was determined to be relatively stable, as neither the bolts nor the steel strips displayed any signs of damage. However, the steel strips of M_4 did little to inhibit CFRP debonding. Indeed, the debonding of the CFRP strips could easily extend beyond the steel anchorage strips, especially during the interfacial debonding caused by shear bending cracks, and eventually lead to beam damage. For the remaining evaluated anchoring methods, the behaviour of the CFRP anchorage strips was relatively unstable. In the process of CFRP strip debonding caused by central beam bending cracks and bending shear cracks, the anchorage strips were observed to debond as well, causing failure. Because the process of CFRP interface debonding resulting from central beam bending shear cracks is complex, and the debonding failure of anchorage strips is relatively straightforward, this paper presents the CFRP load–strain curves for the slab specimens under third-point loading in Fig. 9. The data used in Fig. 9 is the tensile strain in the CFRP strengthening on the bottom of the slab specimens at the edge of the anchorage strips near the support and at midspan.

As shown in Fig. 9(a), when anchored in concentration by adhesive, the change trend in the tensile strains in the different locations of the CFRP strips were similar: the strips appeared to distribute the load and resisted CFRP debonding failure. As shown in Fig. 9(b), when anchored in intervals by adhesive, the change trend in the tensile strain of the

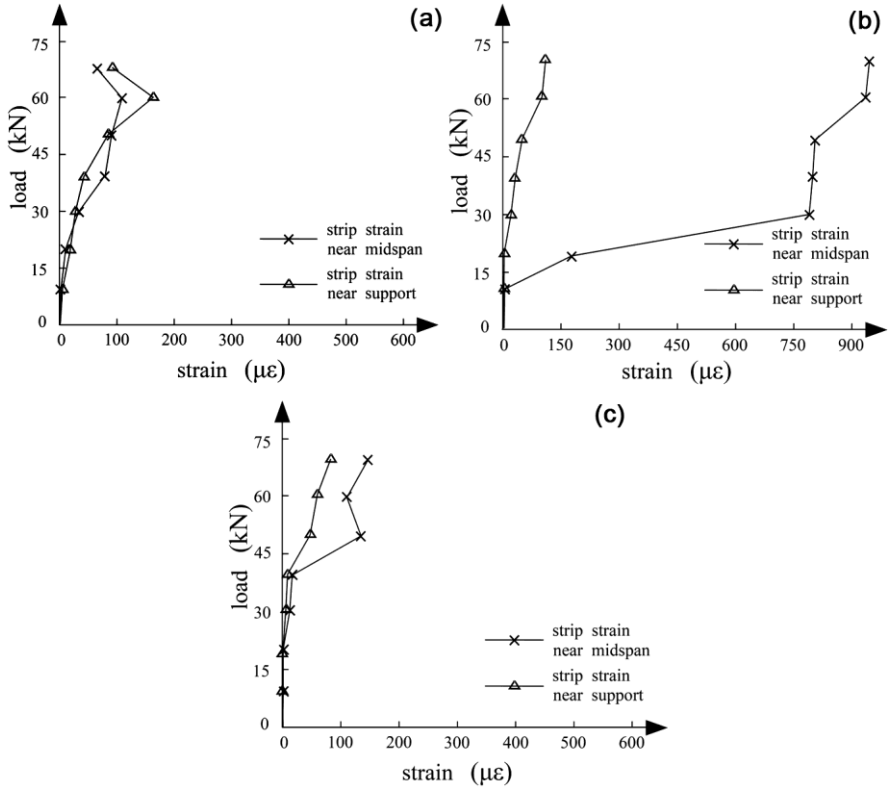

Fig. 9 — CFRP load–strain curves on the (a) M_1 side of S_1, (b) M_2 side of S_1 and (c) M_3 side of S_2.

CFRP strips was obviously different: near the midspan of Slab S1, the CFRP strips carried a larger tensile strain than near the support, causing the strips to debond. This indicates that anchoring CFRP strips in intervals by adhesive provided a lesser degree of load distribution along the primary strengthening strips. As a result, during interfacial debonding caused by bending shear cracks, CFRP debonding could easily extend beyond the anchorage strips along the primary strengthening and eventually result in beam failure. As shown in Fig. 9(c), under concentrated closed-looped adhesive anchoring, the change trend in the tensile strain of the primary CFRP strengthening strips exhibited no difference: the CFRP strips had the ability to coordinate work and resist the destruction of CFRP debonding.

The behaviours of the four anchoring methods evaluated in this study are summarized in Table 2. Overall, anchoring in intervals with adhesive resulted in a significant increase in the likelihood of debonding failure in the slab specimens, and accordingly the ductility of slab specimens was generally poor.

As longitudinal cracks readily appear in T-beams, which are loaded in a similar fashion as the experimental slab, T-beam CFRP strengthening should be anchored according to method M1. Though the slabs of box beam bridges are more complex than those of T-beam bridges, they are still loaded in a fashion similar to the experimental slab, so box beam CFRP strengthening should also be anchored according to method M1. Despite these recommendations, anchoring experiments should be conducted on specimens similar to the strengthening target to determine the optimal anchoring method.

5 Flexural Reinforcement and Anchorage Theory of Bridge Deck Strengthening

5.1 Existing Anchorage Theory

The requirements of the strengthening design code for highway bridges (JTG/TJ22-2008) stipulate that for a concrete slab, at least two anchor strips must be set perpendicularly to CFRP bearing fibres, evenly spaced within the extended length of the anchorage beyond the strengthening zone, where one of the strips must be set at the end of the extended length. The width and thickness of each strip should not be less than half of the primary strengthening strip width and thickness, respectively. The slab specimens tested in this paper were designed in accordance with these requirements. However, there is no clear specification regarding the application of bridge deck anchorage reinforcement theory, representing a clear need for improvement, accordingly proposed in this section.

5.2 Anchorage Theory of Bridge Deck Strengthening

The effective bridge deck strengthening length l_{eff} is the length of CFRP l_{CFRP} minus the extended anchorage length at each end l_a [21]. The equation describing the required extended anchorage length is as follows:

$$l_a = 2\sqrt{\frac{E_{CFRP}\, t_{CFRP}}{\sqrt{f_{cu}}}} \qquad \ldots(1)$$

Analyses of the interfacial stress between the CFRP and concrete structure usually adopt the assumption of elastic deformation. According to Smith and Teng [22], the analytical solution for the interfacial and normal shear stress between CFRP and concrete in CFRP strengthened beams under load is given by:

$$\tau(x) = m_1 V(x) + \frac{m_2}{\lambda} M(0) e^{-\lambda x} + \tau^*(x) \qquad \ldots(2)$$

where:

$$\lambda^2 = \frac{G_a b_p}{t_a}\left[\frac{(y_c + y_p)(y_c + y_p + t_a)}{E_c I_c} + \frac{1}{E_c A_c} + \frac{1}{E_p A_p}\right]$$

$$m_1 = \frac{G_a}{t_a} \cdot \frac{1}{\lambda^2}\left(\frac{y_c + y_p}{E_c I_c + E_p I_p}\right)$$

Table 2 — Comparison of ultimate stress in CFRP strips for different anchoring methods.

Specimen	Debonding location	Debonding mode	Ultimate stress in CFRP strips (MPa)	Utilization of CFRP capacity (%)
D_1	M_2 side	Debonding beyond CFRP strips, slab damage	1369	59.52
D_2	M_4 side	Debonding within CFRP strips, CFRP strips fractured, slab damage	1527	66.39
S_1	M_2 side	Debonding beyond CFRP strips, slab damage	1319	57.35
S_2	M_4 side	Debonding beyond CFRP strips, slab damage	1784	77.56

$$m_2 = \frac{G_a}{t_a} \cdot \frac{y_c}{E_c I_c}$$

$$\tau^*(x) = -m_1 pch(\lambda x) e^{-k}$$

$$K = \lambda(B-a)$$

where b_p is the CFRP strip width on the bottom of the slab specimen; T_a is the thickness of the adhesive layer; A, E, I, and G are the cross-sectional area, elastic modulus, moment of inertia, and shear modulus, respectively, where the subscripts c, p, and a represent the concrete beam, CFRP, and adhesive layer, respectively; y_c represents the distance from the slab specimen section centre to the bottom of the slab; y_p represents the distance from the CFRP section centre to the bottom of the slab; the coordinate x indicates the distance of the evaluated section from the end of the CFRP strip; $V_{(x)}$ represents for shear force at the evaluated section at x; $M_{(0)}$ is the bending moment at the end of the CFRP strengthening; a is the distance from the support to the end of the CFRP strengthening strip; and B is distance from the support to the concentrated load P.

The solution for the interfacial normal stress of a bridge deck under load is:

$$\sigma_y(x) = e^{-\beta x}[C_1 \cos(\beta x) + C_2 \sin(\beta x)] - n_1 \frac{d\tau(x)}{dx} - n_2 q \quad \ldots(3)$$

where:

$$\beta = \sqrt[4]{\frac{E_a b_p}{4t_a}\left(\frac{1}{E_c I_c} + \frac{1}{E_p I_p}\right)}$$

$$n_1 = \left(\frac{y_c E_p I_p - y_p E_c I_c}{E_c I_c + E_p I_p}\right)$$

$$n_2 = \frac{E_p I_p}{b_p(E_c I_c + E_p I_p)}$$

$$C_1 = \frac{E_a}{2\beta^3 t_a}[V(0) + \beta M(0)] - \frac{n_3}{2\beta^3}\tau(0) + \frac{n_1}{2\beta^3}\left[\frac{d^4\tau(x)}{dx^4}\bigg|_{x=0} + \beta \frac{d^3\tau(x)}{dx^3}\bigg|_{x=0}\right]$$

$$C_2 = -\frac{E_a}{2\beta^2 t_a} \cdot \frac{1}{E_c I_c} M(0) - \frac{n_1}{2\beta^2} \cdot \frac{d^3\tau(x)}{dx^3}\bigg|_{x=0}$$

The analytical solution for the distribution of interfacial shear stress and normal stress in the slab specimens under the elastic deformation as per Smith and Teng [22] is given in Fig. 10, which shows that the peak of interfacial normal stress and shear stress in the slab specimens happens near the end of the CFRP strips in the elastic deformation, while the interfacial normal stress and shear stress far from the ends of the CFRP strips tends to zero.

The ultimate stress at the end interface of the CFRP can be determined by the Culon–Morper rule:

$$\tau(x) + \sigma_y(x)\tan\varphi \le C \quad \ldots(4)$$

where, φ is the internal friction angle of the adhesive layer and C is the adhesion of the adhesive layer.

When the anchorage strips were concentrated and attached using adhesive on the end of the CFRP strengthening strips and met the requirements of the anchorage length, they were able to effectively restrain CFRP debonding, improving the capacity of the slab specimens. If the strips were anchored in intervals by adhesive on the end of the CFRP strengthening, a portion of the interfacial normal and

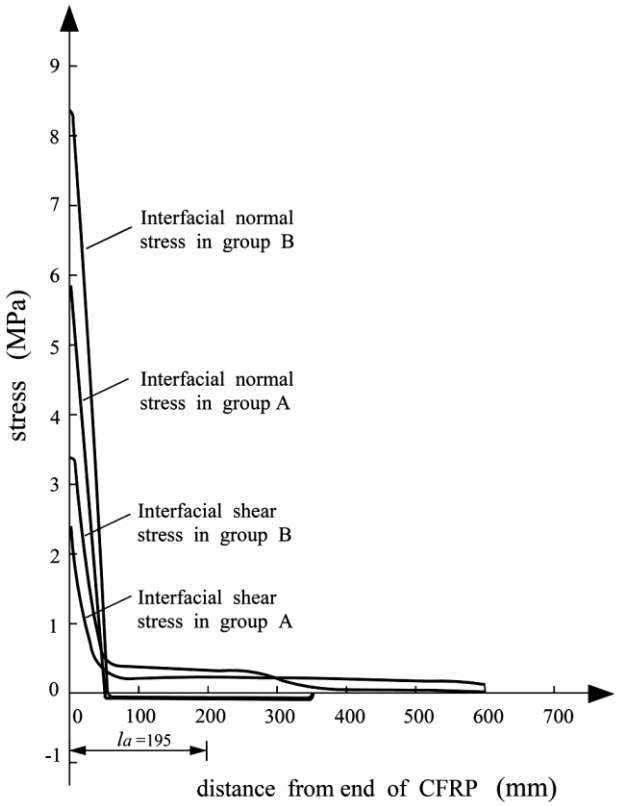

Fig. 10 — Interfacial shear stress and normal stress distribution in the slab specimens under elastic deformation.

shear stress could not be effectively restrained, promoting the development of central stress bending cracks, interfacial debonding caused by bending shear cracks, and debonding beyond the anchorage strips, resulting in structural damage. Slab failure indeed occurred during the experiments on the side with the anchorage consisting of strips attached in intervals by adhesive, verifying this conclusion.

As illustrated by the shear stress distribution at the beam end in Fig. 10, the anchorage length should take a safety factor into account. By synthesizing the crack distribution shown in Fig. 5 with the strain distribution shown in Fig. 8, a safety factor of 1.5 was identified. Note that the anchorage length of CFRP l_a is different for different slab spans l. As a result, Eq. (1) for l_a should be modified as:

$$l_a = 1.07 \cdot l \sqrt{\frac{E_{CFRP} t_{CFRP}}{\sqrt{f_{cu}}}} \quad \ldots(5)$$

In summary, because the spans of T-beam bridges are small, and accordingly the distance between the two inflection points is short, when strengthening T-beam bridge slabs with CFRP, it is best to anchor the strengthening strips with open concentrated CFRP strips attached by adhesive, in which two or more anchorage strips are set edge to edge in the centre of the anchorage extension. With respect to the other anchoring methods, T-beam bridge slabs are not effectively strengthened when anchored with closed-looped concentrated CFRP strips attached with adhesive. Therefore, this method should not be used for strengthening strip anchorage, but possibly to strengthen slabs near the expansion joints of T-beam bridges. Because anchoring with steel strips is likely to damage a T-beam bridge slab, is difficult to install, and provides a poor anchoring effect, this anchoring method is not recommended for use. Because the spans of a box girder bridge slab are larger, and accordingly the distance between two inflection points is longer, when strengthening box girder bridge slabs with CFRP strips, in addition to the requirements stated above, a greater quantity of evenly spaced anchorage strips should be provided.

6 Conclusions

Rectangular concrete slabs strengthened with CFRP strips were tested to simulate the strengthening of T-beam and box-girder decks against longitudinal cracking. Using the results of static load experiments, the effects of four different CFRP strip anchoring methods were compared. The conclusions were:

(i) Cracks observed during the experiments and the measured CFRP strain distribution showed that the open concentrated CFRP strips attached by adhesive and closed-looped concentrated CFRP strips attached by adhesive are more effective than the open CFRP strips attached in intervals by adhesive and steel strips attached with bolts.

(ii) Debonding of the CFRP from the slab specimens occurred from the side of the slab where the strengthening was anchored with open CFRP strips attached in intervals by adhesive, indicating poor performance of this anchoring method. Indeed, under this anchoring method, the ductility of the slab specimen was quite low due to debonding.

(iii) When strengthening T-beam bridge slabs with CFRP, the strengthening should be anchored by open concentrated CFRP strips set edge-to-edge and attached by adhesive, and more than two anchorage strips on each end should be centred within the anchorage extension.

(iv) When strengthening box girder bridge slabs with CFRP, the previous conclusion is also valid, but the number of strips should be increased.

Note that the results in this paper are based on scale model tests, so the data may be of limited validity when applied to full scale slabs. Because dimensions of the experimental slabs are closer to those of a T-beam, scale has much less influence on experimental results applied to T-beams, so the data is more representative of T-beam slab behaviour. Further research is required to capture any influence of scale on the outcome of this study, particularly with regard to box-beam slabs. Additionally, further research could investigate the effects of the simple-span assumption of continuous slab spans on the effectiveness of the evaluated anchoring methods. In all, this research provides an excellent reference and helpful basis informing the design of CFRP strengthening anchorage for slab spans. The anchorage theory in this paper assumes elastic deformation, which does not completely conform to the limit stress state. Modelling methods will be adopted in the future.

Acknowledgements:

This project was funded by the Talent Training Project, Liaoning University of Science and Technology, China. (2019RC01).

References

1 Deshan W, Shuirong G & Jiny J, *J Chin Fore Highway*, 32.1 (2012) 179（in Chinese）.

2 Jianchu H, Fangcheng M & Jun Z, *World Bridges*, 46.2 (2018) 74（in Chinese）.

3 Weizu T, *World Bridges*, 3 (2003) 53（in Chinese）.

4 Biliang C, Jiwen Z & Chuanyao W, *Sci Tech Eng*, 13.14 (2013) 4120（in Chinese）.

5 Ling X, Shuai T, Tong Z & Lingling J, *J Wuhan Univ Technol*, 35.6 (2013) 70（in Chinese）.

6 Lipeng X, Yu Z, *J Dong Guan Univ Technol*, 23.1 (2016) 80（in Chinese）.

7 Xin Y , Wei Z, *Highway*, 6 (2017) 99（in Chinese）.

8 Nawal K, Ramanjaneyulu K, *Constr Build Mater*, 201 (2019) 746.

9 Nawal K, Ramanjaneyulu K, *Constr Build Mater*, 137 (2017) 520.

10 Yail J K, Seung W H , Jae Y K *et al.* , *Eng Struct*, 79 (2014) 256.

11 Toshihiko N, Takeharu T, *Construct Eng Pros*, 63A (2017) 1263（in Japanese）.

12 Lichen W, Jinyuan Z , Jie Xu *et al.*, *Constr Build Mater*, 160 (2018) 82.

13 Junyan X, Guibing L & Binbin Z, *Safety Scie J*, 28. 6 (2018) 122（in Chinese）.

14 Xin Y, Jiwen Z & Shoutan S, *Construct Techno*, 378 (2012) 19（in Chinese）.

15 Jinguang T, Jianfei C & Smith S T, *Reinforced concrete structure with FRP*(China Building Industry Press, China), 2005（in Chinese）.

16 Elgabbas F, El-Ghandour A A, Abdelrahman A A & El-Dieb A S, *Compos Struct*, 8 (2009) 401.

17 Robert K, Albin K & Thomas K, *Eng Struct*, 7 (2014) 283.

18 Çelebi M, Özgür A & Cengizhan D, *Constr Build Mater*, 7 (2016) 553.

19 João G, Jorge M P, João G F & António S G, *Constr Build Mater* , 8 (2017) 56.

20 *Code for Design of Highway Reinforced Concrete and Prestressed Concrete Bridges and Culverts in China (JTG D62-2004)* (China Communications Press, China) 2004（in Chinese）.

21 Smith S T & Jinguang T, *Eng Struct*, 4 (2002) 397.

22 Smith S T & Jinguang T, *Eng Struct*, 7 (2001) 857.